NJC

Synthesis and crystal structure of nitrosoruthenium complexes cis-[Ru(NO)Py$_2$Cl$_2$(OH)] and cis-[Ru(NO)Py$_2$Cl$_2$(H$_2$O)]Cl. Photoinduced transformations of cis-[Ru(NO)Py$_2$Cl$_2$(OH)]†

Alexander N. Makhinya,*[ab] Maxim A. Il'in,[ab] Ruslan D. Yamaletdinov,[a] Ilya V. Korolkov[ab] and Iraida A. Baidina[a]

The interaction of K$_2$[Ru(NO)Cl$_5$] with an excess of pyridine followed by concentration of the reaction solution afforded two crystalline modifications of cis-[Ru(NO)Py$_2$Cl$_2$(OH)] (**1a** and **1b**). The treatment of this hydroxocomplex with hydrochloric acid gave an aquacomplex cis-[Ru(NO)Py$_2$Cl$_2$(H$_2$O)]Cl (**2**). The prepared complexes were characterized by elemental analysis, X-ray diffraction, infrared and ^{1}H NMR spectroscopies. Infrared and Raman spectroscopies provided evidence that irradiation of cis-[Ru(NO)Py$_2$Cl$_2$(OH)] ($\lambda \sim$ 450 nm, T = 80 K) resulted in photoisomerization with the formation of metastable states MS1 (isonitrosyl complex) and MS2 (η^2-coordination of the NO). The population of the MS1 state amounts to 60%. Differential scanning calorimetry (DSC) was used to determine the activation parameters for MS1: E_a = 65.2(3) kJ mol^{-1}, k_0 = 1.05(7) $\times$ 10^{14} s^{-1}. These experimental data agree well with DFT calculations.

Introduction

The interest in the chemistry of nitrosocomplexes of ruthenium is currently stimulated by two major items. On the one hand, due to the intrinsic presence of the NO group, these compounds are physiologically active and are considered as sources/regulators of the content of nitrogen monooxide in biological systems.[1] On the other hand, they are capable of light-induced isomerization affording compounds in which the nitrosyl group is bound either through the oxygen atom (MS1) or through both oxygen and nitrogen in a bidentate side-on arrangement (MS2).[2] This makes them promising for the design of nitrosoruthenium-based hybrid materials combining photochromic properties with electroconductivity or magnetism.[3]

Among known ruthenium nitrosocomplexes, the largest population of the metastable states is demonstrated by [Ru(NO)Py$_4$Cl](PF$_6$)$_2$·0.5H$_2$O ($\sim$92% for MS1 and $\sim$48% for MS2).[4] Recent studies on the photoisomerization of another ruthenium nitrosocomplex cis-[Ru(NO)(NO$_2$)$_2$Py$_2$(OH)]·2H$_2$O has revealed that the population of the MS1 state is 66–75%.[5] Other nitrosopyridine complexes of ruthenium lack photochemical examination,
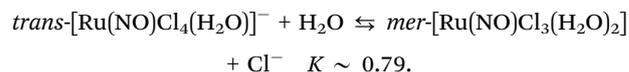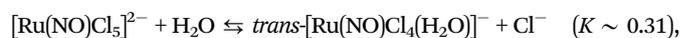
which can be related to insufficient information on effective synthetic methods, structural features and reactivity of these compounds.

The purpose of this study was the development of synthetic approaches to novel nitrosoruthenium complexes of the cis-dipyridine series, determination of their crystal structure, as well as investigation of photoisomerization of cis-[Ru(NO)Py$_2$Cl$_2$(OH)].
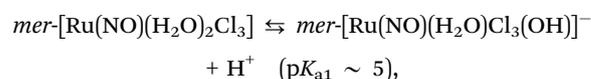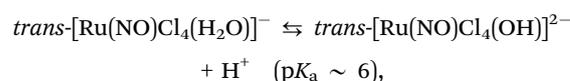
Results and discussion

Synthesis

Our experiments give evidence that heating K$_2$[Ru(NO)Cl$_5$] with an excess of pyridine in the absence of a solvent has no effect. In an aqueous solution the ion [Ru(NO)Cl$_5$]$^{2-}$ on heating undergoes aquation:[6]

$$[Ru(NO)Cl_5]^{2-} + H_2O \leftrightarrows trans\text{-}[Ru(NO)Cl_4(H_2O)]^- + Cl^- \quad (K \sim 0.31),$$

$$trans\text{-}[Ru(NO)Cl_4(H_2O)]^- + H_2O \leftrightarrows mer\text{-}[Ru(NO)Cl_3(H_2O)_2] + Cl^- \quad K \sim 0.79.$$

The resulting aquachlorocomplexes are weakly acidic:[6,7]

$$trans\text{-}[Ru(NO)Cl_4(H_2O)]^- \leftrightarrows trans\text{-}[Ru(NO)Cl_4(OH)]^{2-} + H^+ \quad (pK_a \sim 6),$$

$$mer\text{-}[Ru(NO)(H_2O)_2Cl_3] \leftrightarrows mer\text{-}[Ru(NO)(H_2O)Cl_3(OH)]^- + H^+ \quad (pK_{a1} \sim 5),$$

[a] Nikolaev Institute of Inorganic Chemistry, 3 Acad. Lavrentiev Ave., Novosibirsk, 630090, Russia. Web: www.niic.nsc.ru

[b] Novosibirsk State University, 2 Pirogova Str., Novosibirsk, 630090, Russia. E-mail: sas.fen@mail.ru; Web: www.nsu.ru

† Electronic supplementary information (ESI) available: Fig. S1–S6, Table S1. CCDC 1055425–1055427. For ESI and crystallographic data in CIF or other electronic format see DOI: 10.1039/c6nj02425d

$$mer\text{-}[Ru(NO)(H_2O)Cl_3(OH)]^- \leftrightarrows mer\text{-}[Ru(NO)Cl_3(OH)_2]^{2-}$$
$$+ H^+ \quad (pK_{a2} \sim 7.5).$$
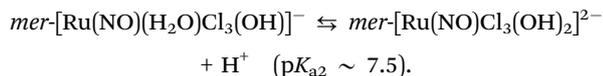
The heating of the saturated aqueous solution of $K_2[Ru(NO)Cl_5]$ with a large excess of pyridine gives a viscous product, which does not afford any crystalline materials. Tentatively, this viscous reaction mixture contains polymeric complex compounds with μ-OH-ions, similar to those forming in the synthesis of nitrosoruthenium ammonia complexes.[8]

When the reaction is carried in nitrosocomplex-poor solutions under a small excess of pyridine, the nitrosopyridine complexes can be isolated (Scheme 1). Under the concentration $C_{Ru} \sim 10^{-1}$ M the reaction solution affords the precipitate of $trans\text{-}[Ru(NO)Py_2Cl_2(OH)]$.[9] Boiling a more diluted solution of $K_2[Ru(NO)Cl_5]$ ($C_{Ru} \sim 10^{-2}$ M) with an excess of pyridine gives $trans\text{-}[Ru(NO)Py_4(OH)]^{2+}$. The concentration of the reaction solution under an excess of chloride ions results in degradation of this tetrapyridine form and the formation of $cis\text{-}[Ru(NO)Py_2Cl_2(OH)]$ (1).

Under heating, $cis\text{-}[Ru(NO)Py_2Cl_2(OH)]$ is partially isomerized in the $trans$-isomer. We employed the much better solubility of the cis-isomer in DMF for separation of this mixture.

On interaction of an aqueous solution of $cis\text{-}[Ru(NO)Py_2Cl_2(OH)]$ with concentrated hydrochloric acid at room temperature, the coordinated hydroxide ions are protonated. Slow evaporation of this reaction mixture yields the crystals of 2.

Crystal structures of $cis\text{-}[Ru(NO)Py_2Cl_2(OH)]$ (1a and 1b)

The structures of 1a and 1b are built from the neutral complex moieties $cis\text{-}[Ru(NO)Py_2Cl_2(OH)]$. The structures of the coordination entities presented in thermal ellipsoids together with atomic labeling are illustrated in Fig. 1; selected bond lengths and angles are listed in Table 1. The coordination polyhedron of ruthenium is a slightly distorted octahedron (RuN_3Cl_2O). Bond angles at ruthenium deviate from 90° within 5.3°.

In the coordination entities two pyridine molecules are in the cis-position to each other; the equatorial square is complemented with two chloride ions. The coordination geometry in the crystals
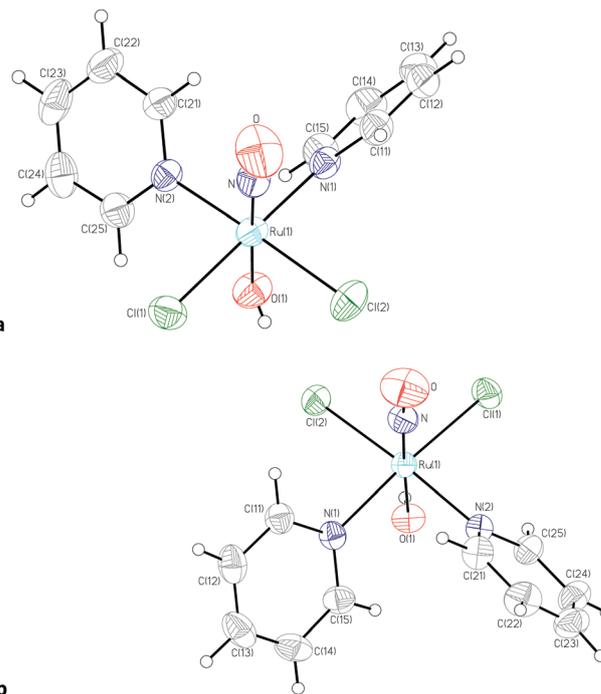

a

b

Fig. 1 The structure of the complex particle $cis\text{-}[Ru(NO)(Py)_2Cl_2(OH)]$ (in 1a and 1b).

of 1a and 1b is somewhat different; the largest discrepancy of ~ 0.01 Å is observed for the lengths of the bonds N–O and Ru–O; the average $Ru-N_{Py}$, Ru–Cl and Ru–N distances are similar in these crystalline modifications. The lengths of the bonds Ru–Cl fall within the range 2.36–2.38 Å, characteristic of amine nitrosoruthenium complexes having the chloride ion in the $trans$-position to the molecule of the amine.[10] In 1a the bond angle O–N–Ru of $\sim 172.9°$ deviates from the ideal value much more than in 1b ($\sim 177.2°$); however, such differences were noticed in the nitrosocomplexes several times.[11] The pyridine molecules are tilted to the equatorial plane by $\sim 50°$. In the complex particles, the central atom Ru is displaced from the equatorial plane towards the NO-group by 0.08 Å (1a) and 0.1 Å (1b).

In the crystals of 1a and 1b the coordination moieties are joined by short contacts Cl···H–C, the distance Cl···H between the coordinated chloride ions and pyridine hydrogens is ~ 2.8 Å; the shortest separations Ru···Ru in the structures are ~ 6.9 and 5.9 Å, respectively. The packing of the structural units in the crystals of 1a and 1b is shown in Fig. S1 (see ESI†).

Crystal structure of $cis\text{-}[Ru(NO)Py_2Cl_2(H_2O)]Cl$ (2)

The structure comprises complex cations $cis\text{-}[Ru(NO)Py_2Cl_2(H_2O)]^+$ and Cl^- anions. The structure of the coordination entities presented in thermal ellipsoids together with atomic labeling is illustrated in Fig. 2; selected bond lengths and angles are listed in Table 1.

The central Ru atom has a slightly distorted octahedral environment. The $trans$-position to the nitrosogroup is occupied with a water molecule. The length of the bond $Ru-N_{NO}$ is ~ 1.73 Å, and for N–O it is ~ 1.14 Å. The average distance $Ru-N_{(Py)}$ is ~ 2.10 Å.
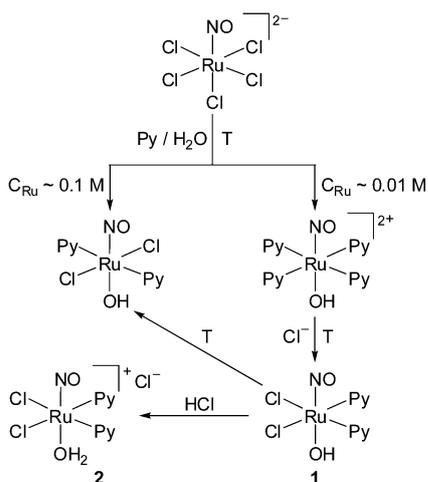
Scheme 1 Interaction of diluted aqueous solutions of $K_2[Ru(NO)Cl_5]$ with an excess of pyridine.

Table 1 Main interatomic distances and angles in the structures of **1a**, **1b** and **2**

Distances [Å]	1a	1b	2	Distances [Å]	1a	1b	2
Ru(1)–N	1.752(2)	1.750(1)	1.729(1)	Ru(1)–Cl(1)	2.3841(9)	2.3727(5)	2.3611(4)
Ru(1)–O(1)	1.952(2)	1.933(1)	2.041(1)	Ru(1)–Cl(2)	2.3625(7)	2.3759(5)	2.3630(5)
Ru(1)–N(1)	2.102(2)	2.105(1)	2.102(1)	N–O	1.138(3)	1.149(2)	1.140(2)
Ru(1)–N(2)	2.097(2)	2.097(1)	2.104(1)				

Angles [°]	1a	1b	2	Angles [°]	1a	1b	2
N–Ru(1)–O(1)	178.7(1)	177.04(6)	176.48(6)	N(2)–Ru(1)–Cl(2)	174.73(6)	174.97(4)	174.71(4)
N–Ru(1)–N(1)	92.42(9)	94.49(6)	90.92(6)	N(2)–Ru(1)–N(1)	89.55(8)	87.93(5)	91.13(5)
N–Ru(1)–N(2)	95.32(9)	91.52(6)	95.29(6)	O(1)–Ru(1)–Cl(1)	89.36(7)	88.39(4)	87.32(3)
N–Ru(1)–Cl(1)	91.04(7)	91.82(5)	96.26(5)	O(1)–Ru(1)–Cl(2)	88.84(7)	89.80(4)	89.98(5)
N–Ru(1)–Cl(2)	89.92(7)	93.15(5)	89.95(5)	Cl(1)–Ru(1)–Cl(2)	91.16(3)	91.07(2)	91.33(2)
N(1)–Ru(1)–Cl(1)	176.46(6)	173.57(4)	172.77(4)	O(1)–Ru(1)–N(1)	87.21(9)	85.25(5)	85.56(5)
N(1)–Ru(1)–Cl(2)	89.63(6)	89.83(4)	89.57(3)	O(1)–Ru(1)–N(2)	85.92(9)	85.52(5)	84.85(5)
N(2)–Ru(1)–Cl(1)	89.35(6)	90.66(4)	87.26(3)	O–N–Ru(1)	172.9(2)	177.2(1)	174.8(1)
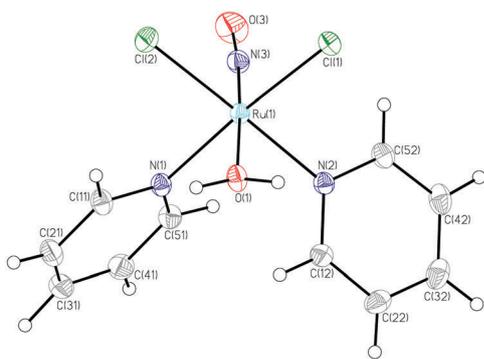
Fig. 2 The structure of the complex particle in **2**.

The geometry of the O–N–Ru fragment is close to linear (175.0°), and bond angles at the Ru atom deviate from 90° by not more than by 6.3°. The ruthenium atom is shifted from the equatorial plane by ~0.1 Å. The pyridine molecules make a tilt to the equatorial plane of ~50°.

In the structure of **2** the coordinated water molecules form hydrogen bonds to the uncoordinated chloride ions with a O···Cl distance ~2.95 Å. The uncoordinated chloride ions make short contacts to the nitrosogroup with the O···Cl distance ~3.24 Å. The shortest separations between the ruthenium atoms in the structure are 7.04–7.51 Å. The packing of the structural units in **2** is illustrated in Fig. S2 (ESI†).

Photoinduced transformation of *cis*-[Ru(NO)Py$_2$Cl$_2$(OH)] and calculation of metastable states

The optimized geometries for the different states are given in Table S1 (ESI†). The theoretical geometry of the GS matches the experimental data; slight discrepancies can be attributed to the influence of the crystalline environment neglected in the calculations. It is worth noting that the length of the bond Ru–NO in MS1 (1.883 Å) and TS1 (2.268 Å) is enlarged as compared to the GS (1.774 Å), while other parameters are hardly touched and correlate with literature data. In our calculations, the lengths of Ru–N$_{(Py)}$ bonds (2.15–2.17 Å) are similar to the Ru–amine bond length (for example, 2.05–2.14 Å for tetraazamacrocycle).[12] Elongation of the Ru–NO bond

accompanied an increasing total energy. This is caused by a decrease of the Ru–NO bond energy. Andriani *et al.*[13] demonstrated depopulation of π and σ orbitals Ru–NO by 3.67–3.95 and 1.63–1.96 times respectively for GS/MS1. Also in the Raman spectrum, we found that ν(Ru–ON) < ν(Ru–NO), and so we can say there is a decrease of Ru–NO bonding in MS1 relatively to GS bonding. The same result was obtained by the theoretical investigation performed by Andriani *et al.*[14] This effect is especially expressed in transition state TS1. This observation can be assigned to a pre-requisite breakage of the bond Ru–ON on thermal decay of MS1. Also, in our calculations there are only singlet states as a ground electron state for GS and MS1 (a well-known result)[15] for TS1.

IR spectra of the ground state of *cis*-[Ru(NO)Py$_2$Cl$_2$(OH)] exhibit intensive bands of stretching vibrations ν(NO) at 1832 (for **1a**) and 1825 (for **1b**) cm^{-1}. These values fall within the range characteristic of the majority of ruthenium nitrosocomplexes containing the diamagnetic center Ru(II) and the linearly coordinated group NO$^+$.[16] After irradiation of sample **1b** with visible light (λ = 450 nm, 80 K), the IR spectrum in the range 1500–1850 cm^{-1} (Fig. 3) explicitly demonstrates new bands at 1501 and 1686 cm^{-1}.
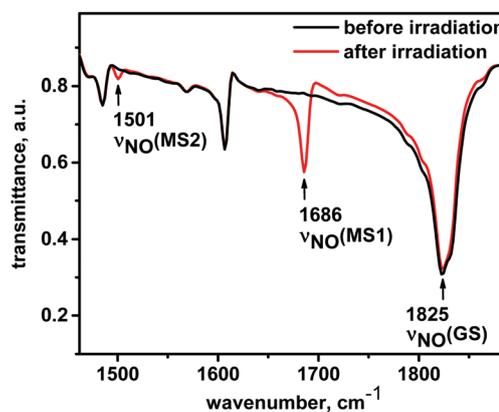
Fig. 3 Infrared spectra of *cis*-[Ru(NO)Py$_2$Cl$_2$(OH)] in the spectral region of the ν(NO) stretching vibrations in the ground state (GS) and after irradiation.

The development of these bands indicates the formation of the metastable isomers MS2 and MS1, respectively.[17] These values of stretching vibrations ν(NO) are comparable with calculated frequencies for ruthenium tetraazamacrocycle nitrosyl complexes with ν(NO) 1891, 1780 and 1576 cm^{-1} for GS, MS1 and MS2, respectively.[12] The decrease in the area of the band ν_{NO} (GS) in IR spectra of the samples irradiated to saturation during 10 min was used for an assessment of the population of MS1. In three parallel runs the maximum population was about 60%.

Raman spectra of the irradiated samples also show some evolution (Fig. 4). After irradiation of the sample with a laser (λ = 457 nm) within the spectral range 400–600 cm^{-1}, a new intensive band appears at 437 cm^{-1}, which corresponds to symmetric vibrations ν(Ru–ON) of the state MS1. The intensity of the band at 573 cm^{-1}, corresponding to the vibrations ν(Ru–NO) in the ground state (GS), is significantly diminished. The vibration ν(NO) drifts from 1820 (GS) to 1685 cm^{-1} (MS1), as was observed in the IR spectra. The other Raman bands in the spectra of the irradiated and original samples are virtually the same.

The DSC technique was applied to estimate the kinetic parameters of the transition of the metastable state MS1 to the ground state GS. The measurements were carried out for three distinct samples of **1b** at different ramp rates.
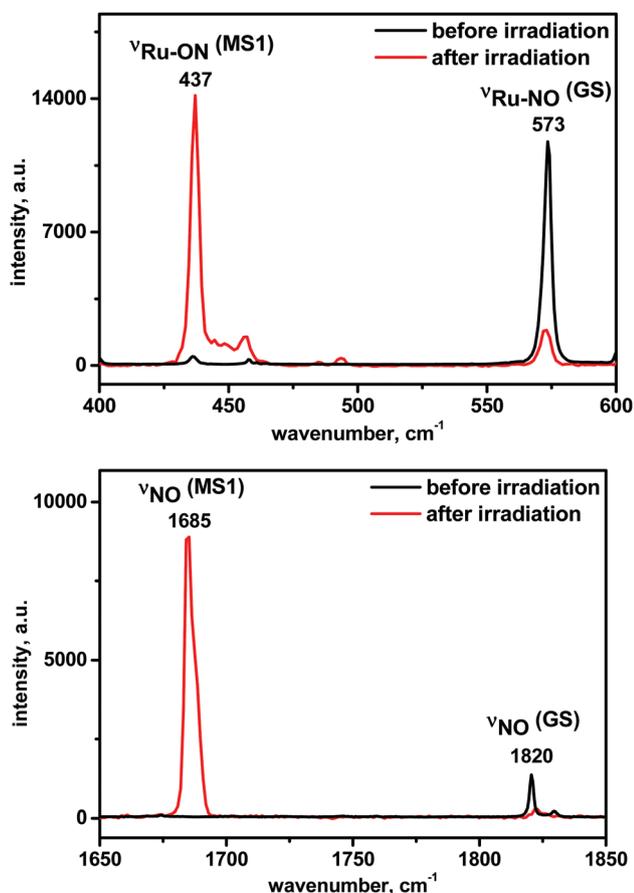

Fig. 4 Raman spectra of *cis*-[Ru(NO)Py$_2$Cl$_2$(OH)] in the spectral region of the ν(Ru–NO) and ν(NO) stretching vibrations in the ground state (GS) and after irradiation.
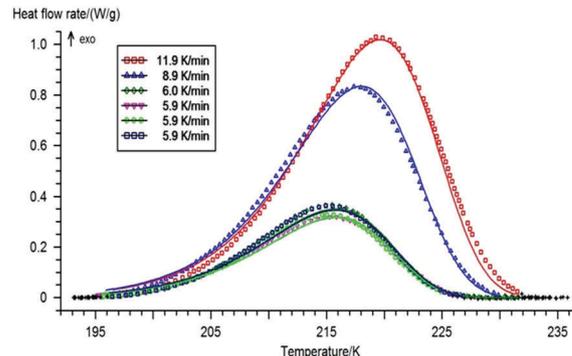

Fig. 5 Calculated (lines) and experimental (dots) DSC curves for *cis*-[Ru(NO)Py$_2$Cl$_2$(OH)].

The resulted dependence of the heat flow on temperature (Fig. 5) is well approximated by first-order kinetics:

$$\dot{H} = H_{tot} \cdot k_0 \cdot \exp\left(-\frac{E_a}{k_B \cdot T} - \frac{k_0}{q}\int_{T_0}^{T} e^{-\frac{E_a}{k_B \cdot T'}} \cdot dT'\right),$$

where $\dot{H}$ is the heat flow, H_{tot} – the overall effect, k_0 – the preexponential factor, E_a – activation energy, q – ramp rate, k_B – the Boltzmann constant, T_0 – the starting temperature.

All the curves were processed within the temperature range 193–237 K, giving E_a and k_0 65.2(3) kJ mol^{-1} and 1.05(7) × 10^{14} s^{-1}, respectively. The value of the activation energy, calculated by DFT as the difference between the TS1 and MS1 energies, was $E_a^{calc.}$ = 66.8 kJ mol^{-1}, in a good accord with the experimental observations. It was suggested earlier,[18] that the decomposition temperature (T_d) of MS1 can be accepted as the value corresponding to the decay rate of 10^{-3} s^{-1}. For the compound under study the result is T_d = 200 K.

Summary and conclusions

Heating of a diluted aqueous solution of K$_2$[Ru(NO)Cl$_5$] ($C_{Ru} \sim$ 0.01 M) with an excess of pyridine affords a solution of the tetrapyridine complex *trans*-[Ru(NO)Py$_4$(OH)]$^{2+}$; its further concentration in the presence of an excess of chloride ions gives *cis*-[Ru(NO)Py$_2$Cl$_2$(OH)]. Depending on the synthetic protocol, we have obtained two crystalline modifications of this complex (**1a** and **1b**). Preparation of the *cis*-isomer of the dipyridine complex by these syntheses in the reactions of substitution for complexes of ruthenium nitrosyl a greater *trans*-effect of molecules Py above the chloride ions is demonstrated. This synthetic approach for obtaining *cis*-isomers is elegant and can be used for the preparation of analogue complexes of ruthenium nitrosyl with other nitrogen heterocyclic bases. The heating of *cis*-[Ru(NO)Py$_2$Cl$_2$(OH)] results in its partial isomerization in the *trans*-isomer, which is less soluble in DMF.

The reaction of the hydroxocomplex (**1a** or **1b**) with concentrated hydrochloric acid at room temperature almost quantitatively affords the aqua complex *cis*-[Ru(NO)Py$_2$Cl$_2$(H$_2$O)]Cl. Similar reactions have previously been discussed in the literature for the other hydroxycomplexes of ruthenium nitrosyl.[8a,9,24]

Table 2 Experimental data and refinement details for **1a**, **1b** and **2**

	1a	1b	2
Formula	$C_{10}H_{11}Cl_2N_3O_2Ru$	$C_{10}H_{11}Cl_2N_3O_2Ru$	$C_{10}H_{12}Cl_3N_3O_2Ru$
Formula weight	377.19	754.38	413.65
Space group	$P2_1/c$	$Pbca$	$Pbca$
a [Å]	15.3824(4)	14.5946(3)	12.4068(3)
b [Å]	6.9222(2)	12.2931(2)	14.0336(3)
c [Å]	14.4655(3)	14.9170(3)	16.9426(4)
β [°]	117.818(1)	90	90
V [Å^3]	1362.28(6)	2676.30(9)	2949.91(12)
Z	4	4	8
R_1 [$I > 2\sigma(I)$]	0.0313	0.0221	0.0226
R_1 (all)	0.0463	0.0408	0.0335

Photochemical studies of *cis*-[Ru(NO)Py$_2$Cl$_2$(OH)] give evidence of the formation of the iso-nitrosyl state Ru–O–N and the state characterized by bi-dentate coordination of NO by the ruthenium atom. According to DSC, the values of the activation energy (E_a) and decomposition temperature (T_d) of MS1 for the complex *cis*-[Ru(NO)Py$_2$Cl$_2$(OH)] (**1b**) amounted to $E_a \sim 65$ kJ mol^{-1} and $T_d \sim 200$ K. These values are close to those of similar *cis*-diaminecomplexes: *cis*-[Ru(NO)Py$_2$(NO$_2$)$_2$(OH)] ($E_a \sim 64$ kJ mol^{-1} and $T_d \sim 206$ K)[5] and *cis*-[Ru(NO)(NH$_3$)$_2$-(NO$_2$)$_2$(OH)] ($E_a \sim 68$ kJ mol^{-1} and $T_d \sim 218$ K).[25] In all these complexes in the *trans*-position to the NO is the OH group. It has been noted many times that a decisive role in the thermal stability of MS1 has the *trans*-ligand to NO.[2,18,26] The population of the iso-nitrosyl state for the complex *cis*-[Ru(NO)Py$_2$Cl$_2$(OH)] (**1b**) is about 60%.

Experimental section

General

The starting K$_2$[Ru(NO)Cl$_5$] was obtained from commercially available ruthenium trichloride hydrate as described in the literature.[6b] Other reagents and solvents were used as purchased and were of chemical grade or better. FT-IR spectra were recorded on a Scimitar FTS 2000 Fourier spectrometer in the range 4000–375 cm^{-1}. The samples were prepared *via* the standard procedure by pressing the compounds in KBr pellets. NMR spectra were recorded on a Bruker Avance 500 spectrometer, w.f. 500.000 MHz (^{1}H), magnetic field strength 11.744 T. The samples were dissolved in DMSO; HMDS was used as the external standard, $\delta(^1$H) = 0.60 ppm. Elemental analyses were performed on a EURO EA3000 (Euro Vector). Determination of Cl was carried out using decomposition by the Shöniger flask combustion method and titration.

Single-crystal structure analysis

Unit cell parameters and intensity data were measured on an automated four-circle X8 APEX Bruker diffractometer (MoKα radiation, graphite monochromator, CCD area detector). The structures were solved by the heavy atom method and refined in the anisotropic approximation; hydrogen atoms were put in idealized positions and refined isotropically. All calculations were performed using SHELXTL.[19]

Crystal data and selected refinement details for **1a**, **1b** and **2** are given in Table 2. CCDC 1055425–1055427 contain the supplementary crystallographic data for this paper.

DFT-calculations

The X-ray results were taken as the initial geometry for GS optimization tasks. It is well known that the metastable states are local minima on the potential energy surface of a non-excited particle.[15] Their geometry was obtained by optimization of a gas-phase particle, with the same sets of atomic coordinates except for the position of the NO group, which was set manually. The transient state (TS) geometry was determined at the corresponding saddle point and verified by frequency analysis. All spin-polarized DFT calculations were carried out using NWChem 6.3[20] by applying B3LYP[21] with pseudopotential for the Ru atom. We have used the following basis sets: 6-31+G(d)[22] – for small atoms; LanL2DZ[23] – for the Ru atom.

Metastable states detection

The data for assessment of the population of the MS1 state were recorded on a Scimitar FTS 2000 Fourier spectrometer in the range 4000–375 cm^{-1}. MS2 was detected at $T = 80$ K with a Nicolet 5700 FTIR spectrometer. The compounds were pressed in KBr pellets, mounted on a copper cold finger with silver paste, and cooled in a closed-cycle vacuum cryostat. KBr windows allowed the irradiation of the KBr sample with light down to a wavenumber of 390 cm^{-1}. The irradiation was performed with a laser with λ = 450 nm (100 mW).

The Raman spectra were recorded with a Horiba LabRAM HR Evolution single spectrometer with a CCD Symphony (Jobin Yvon) detector, which provided 2048 pixels along the abscissa. The laser power at the sample surface was typically 5 mW for the 633 nm line of the He–Ne laser and 0.1 mW for the 457 nm line of the Ar$^+$ laser. The spectra were measured in 180° backscattering collection geometry with a Raman microscope. For measurements, the crystals were wrapped in indium foil for better thermal contact and fixed on the cold finger of a He cryostat. The measurements were performed with spectral resolutions of 1.4 cm^{-1} for the 633 nm line and 2.2 cm^{-1} for the 457 nm line.

A NETZSCH DSC 204 F1 Phoenix differential scanning calorimeter was used to study the kinetics and thermal effects of the reversible photoinduced transition. To study MS1 the

sample was placed in liquid nitrogen vapor and irradiated with a laser (100 mW, 450 nm) for 10 min. The sample was then quickly transferred to a device for DSC. The calorimetric measurements of powdered samples (1–3 mg) were performed in open aluminum crucibles by the heat-flow measurement method at different heating rates of 5.9, 6.0, 8.9 and 11.9 K min^{-1} in a 25 mL min^{-1} Ar flow. To increase the accuracy, the measurements were performed without a supply of gas or liquid nitrogen in the measurement cell during the experiment. The sensitivity calibration of the sample carrier sensors and temperature scale were performed by melting and crystal-to-crystal transition measurements of standard samples (C_6H_{12}, Hg, KNO_3, In). The processing of the experimental data was performed with the Netzsch Proteus Analysis software.

Synthesis of cis-[Ru(NO)Py$_2$Cl$_2$(OH)]

Crystal modification 1a. ~ 1 g (2.6×10^{-3} mol) of $K_2[Ru(NO)Cl_5]$ was dissolved in ~ 200 mL of water and added with ~ 2.6 mL of Py (3.3×10^{-2} mol). The reaction mixture was heated in a boiling water bath for 40 min. Then, ~ 2 g of KCl was added, and the solution was evaporated to dryness. 20 mL of water was added to this mixture, and the solution again evaporated to dryness. After cooling of the reaction mixture to room temperature, 5–10 mL of water was added to dissolve the precipitate (KCl); a relatively insoluble orange precipitate was filtered off. The precipitate was washed with 1 mL of cold water, a minimum amount of ethyl alcohol (1–2 mL) and ether, and dried in a stream of air. To isolate the desired product, the mixture of cis- and trans-isomers was added to ~ 2 mL of DMF at room temperature and filtered, then the filtrate was evaporated to dryness at room temperature. Slow evaporation of the filtrate gave orange crystals of **1a** suitable for X-ray diffraction studies. The yield was about 50%.

Crystal modification 1b. ~ 1 g (2.6×10^{-3} mol) of $K_2[Ru(NO)Cl_5]$ was dissolved in ~ 200 mL of distilled water and added to ~ 2.6 mL of Py (3.3×10^{-2} mol). The reaction mixture was heated in a boiling water bath for 40 min. Then, the resulting mixture was cooled to room temperature, ~ 10 mL of concentrated HCl was added, and the solution was evaporated on a rotary evaporator affording a red oil (at ~ 80 °C). The product was added to 10–20 mL of distilled water and filtered. The filtrate was neutralized by adding 0.7 g of $KHCO_3$ and in one day the orange precipitate of **1b** was filtered. The product was washed with ~ 1 mL of cold water, a minimum amount of ethanol (~ 1 mL) and ether, and dried in a stream of air (yield $\sim 70\%$). Slow evaporation of a solution of **1b** in DMF gave orange crystals of **1b** suitable for X-ray diffraction studies.

IR-spectrum (ν, cm^{-1}; Fig. S3, ESI†): **1a**: 3577 [ν(OH)]; 1832 [ν(NO)]; 1604, 1481, 1448, 1350 [ν(C$_{Py}$–C$_{Py}$), ν(C$_{Py}$–N$_{Py}$)]; 1242, 1209, 1155, 1097, 1066, 1016, 912, 879, 795, 760, 690, 648 [δ(CH)]; 618, 595 [ν(Ru–N$_{NO}$), δ(Ru–NO)]; 569 [δ(Ru–OH)]; 451 [ν(Ru–N$_{Py}$)]; **1b**: 3485 [ν(OH)]; 1825 [ν(NO)]; 1606, 1485, 1452, 1357 [ν(C$_{Py}$–C$_{Py}$), ν(C$_{Py}$–N$_{Py}$)]; 1242, 1213, 1147, 1103, 1070, 1020, 933, 872, 769, 694, 650 [δ(CH)]; 619, 600 [ν(Ru–N$_{NO}$), δ(Ru–NO)]; 571 [δ(Ru–OH)]; 455 [ν(Ru–N$_{Py}$)]. NMR ^{1}H in DMSO (δ, ppm; Fig. S4, ESI†): 8.67 d (4H, H$^{[2,6]}$), 8.08 t (2H, H$^{[4]}$),

7.61 t (4H, H$^{[3,5]}$). Anal. Calcd. for $C_{10}H_{11}N_3O_2Cl_2Ru$, %: C 31.8, H 2.94, N 11.1, Cl 18.8. Found C 31.7, H 2.95, N 11.1, Cl 19.1.

Synthesis of cis-[Ru(NO)Py$_2$Cl$_2$(H$_2$O)]Cl (2)

Concentrated aqueous HCl (~ 0.5 mL) was added dropwise to a solution of 0.1 g of **1a** or **1b** in ~ 10 mL of water. Red crystals of **2**, suitable for X-ray diffraction studies, were obtained by slow evaporation of the resulting solution at room temperature. The product yield is close to quantitative ($\sim 95\%$).

IR-spectrum of **2** (ν, cm^{-1}; Fig. S5, ESI†): 3440, 3171, 2730 [ν(H$_2$O$_{coord}$)]; 1898 [ν(NO)]; 1607, 1489, 1450, 1364 [ν(C$_{Py}$–C$_{Py}$), ν(C$_{Py}$–N$_{Py}$)]; 1242, 1221, 1163, 1070, 1016, 982, 945, 883, 808, 764, 691, 648 [δ(CH)]; 625, 600 [ν(Ru–N$_{NO}$), δ(RuNO)]; 449 [ν(Ru–N$_{Py}$)]. NMR ^{1}H in DMSO (δ, ppm; Fig. S6, ESI†): 8.53 d (4H, H$^{[2,6]}$), 8.20 t (2H, H$^{[4]}$), 7.72 t (4H, H$^{[3,5]}$).

References

1 (a) A. Rathgeb, A. Böhm and M. S. Novak, et al., Inorg. Chem., 2014, **53**, 2718; (b) G. E. Büchel, A. Gavriluta, M. Novak, S. M. Meier, M. A. Jakupec, O. Cuzan, C. Turta, J.-B. Tommasino, E. Jeanneau, G. Novitchi, D. Luneau and V. B. Arion, Inorg. Chem., 2013, **52**, 6273; (c) E. Tfouni, D. R. Truzzi, A. Tavares, A. J. Gomes, L. E. Figueiredo and D. W. Franco, Nitric Oxide, 2012, **26**, 38; (d) J. J. Silva, A. L. Osakabe, W. R. Pavanelli, J. S. Silva and D. W. Franco, Br. J. Pharmacol., 2007, **152**, 112.

2 D. Schaniel, T. Woike and B. Delley, et al., Phys. Chem. Chem. Phys., 2005, **7**, 1164.

3 (a) L. A. Kushch, S. Golhen, O. Cador, E. B. Yagubskii, M. A. Il'in, D. Schaniel, T. Woike and L. Ouahab, J. Cluster Sci., 2006, **17**, 303; (b) D. Schaniel, T. Woike, L. Kushch and E. Yagubskii, Chem. Phys., 2007, **340**, 211.

4 (a) D. Schaniel, B. Cormary, I. Malfant, L. Valade, T. Woike, B. Delley, K. W. Krämer and H. U. Güdel, Phys. Chem. Chem. Phys., 2007, **9**, 3717; (b) B. Cormary, S. Ladeira, K. Jacob, P. G. Lacroix, T. Woike, D. Schaniel and I. Malfant, Inorg. Chem., 2012, **51**, 7492.

5 G. A. Kostin, A. O. Borodin, A. A. Mikhailov, N. V. Kuratieva, B. A. Kolesov, D. P. Pishchur, T. Woike and D. Schaniel, Eur. J. Inorg. Chem., 2015, 4905.

6 (a) E. E. Mercer, W. M. Campbell Jr. and R. M. Wallace, Inorg. Chem., 1964, **3**, 1018; (b) V. A. Emel'yanov, M. A. Fedotov, A. V. Belyaev and S. V. Tkachev, Russ. J. Inorg. Chem., 2013, **58**, 956.

7 V. A. Emel'yanov, I. A. Baidina, S. P. Khranenko, S. A. Gromilov, M. A. Il'in and A. V. Belyaev, J. Struct. Chem., 2003, **44**, 37.

8 (*a*) M. A. Il'yin, V. A. Emel'anov, A. V. Belyaev, A. N. Makhinya, S. V. Tkachev and N. I. Alferova, *Russ. J. Inorg. Chem.*, 2008, **53**, 1070; (*b*) J. E. Earley and T. Fealey, *Inorg. Chem.*, 1973, **12**, 323.

9 A. N. Makhinya, M. A. Il'in, E. V. Kabin, I. A. Baidina, M. R. Gallyamov and N. I. Alferova, *Russ. J. Coord. Chem.*, 2014, **40**, 297.

10 (*a*) B. Serli, E. Zangrando, T. Gianferrara, L. Yellowleesc and E. Alessio, *Coord. Chem. Rev.*, 2003, **245**, 73; (*b*) A. N. Makhinya, M. A. Il'in, I. A. Baidina, P. E. Plyusnin and M. R. Gallyamov, *J. Struct. Chem.*, 2014, **55**, 682; (*c*) M. A. Il'in, V. A. Emel'yanov, I. A. Baidina, N. I. Alferova and I. V. Korol'kov, *Russ. J. Inorg. Chem.*, 2007, **52**, 62.

11 (*a*) H. Nishimura, H. Matsuzawa, T. Togano, M. Mukaida, H. Kakihana and F. Bottomley, *J. Chem. Soc., Dalton Trans.*, 1990, 137; (*b*) G. Tamasi and R. Cini, *J. Mol. Struct.*, 2013, **1048**, 27; (*c*) A. Kumar, R. Pandey, R. K. Gupta, K. Ghosh and D. S. Pandey, *Polyhedron*, 2013, **52**, 837.

12 G. F. Caramomori, A. G. Kunitz, K. F. Andriani, F. G. Doro, G. Frenking and E. Tfouni, *Dalton Trans.*, 2012, **41**, 7327.

13 K. F. Andriani, G. F. Caramori, A. Muñoz-Castro and F. G. Doro, *RSC Adv.*, 2015, **5**, 69057.

14 K. F. Andriani, G. F. Caramori, F. G. Doro and R. L. T. Parreira, *RSC Adv.*, 2014, **43**, 8792.

15 P. Coppens, I. Novozhilova and A. Kovalevsky, *Chem. Rev.*, 2002, **102**, 861.

16 (*a*) E. E. Mercer, W. A. McAlister and J. R. Durig, *Inorg. Chem.*, 1966, **5**, 1881; (*b*) M. J. Rose and P. K. Mascharak, *Coord. Chem. Rev.*, 2008, 2093.

17 (*a*) T. Woike, H. Zöllner, W. Krasser and S. Haussühl, *Solid State Commun.*, 1990, **73**, 149; (*b*) M. E. Chacón Villalba, J. A. Guìda, E. L. Varetti and P. J. Aymonino, *Inorg. Chem.*, 2003, **42**, 2622.

18 K. Ookubo, Y. Morioka, H. Tomizawa and E. Miki, *J. Mol. Struct.*, 1996, **379**, 241.

19 G. M. Sheldrick, *Acta Crystallogr., Sect. A: Found. Crystallogr.*, 2007, **64**, 112.

20 M. Valiev, E. J. Bylaska, N. Govind, K. Kowalskia, T. P. Straatsmaa, H. J. J. Van Dama, D. Wanga, J. Nieplochaa, E. Aprab, T. L. Windusc and W. A. de Jong, *Comput. Phys. Commun.*, 2010, **181**, 1477.

21 (*a*) A. D. Becke, *J. Chem. Phys.*, 1993, **98**, 5648; (*b*) C. Lee, W. Yang and R. G. Parr, *Phys. Rev. B: Condens. Matter Mater. Phys.*, 1988, **37**, 785; (*c*) P. J. Stephens, F. J. Devlin, C. F. Chabalowski and M. J. Frisch, *J. Phys. Chem.*, 1994, **98**, 11623.

22 (*a*) R. Krishnan, J. S. Binkley, R. Seeger and J. A. Pople, *J. Chem. Phys.*, 1980, **72**, 650; (*b*) T. Clark, J. Chandrasekhar and P. V. R. Schleyer, *J. Comput. Chem.*, 1983, **4**, 294; (*c*) J.-P. Blaudeau, M. P. McGrath, L. A. Curtiss and L. Radom, *J. Chem. Phys.*, 1997, **107**, 5016.

23 P. J. Hay and W. R. Wadt, *J. Chem. Phys.*, 1985, **82**, 270.

24 V. A. Emel'yanov, I. A. Baidina, M. A. Il'in and S. A. Gromilov, *J. Struct. Chem.*, 2006, **47**, 380.

25 V. Vorobyev, G. A. Kostin, N. V. Kuratieva and V. A. Emelyanov, *Inorg. Chem.*, 2016, **55**, 9158.

26 D. V. Fomitchev and P. Coppens, *Comments Inorg. Chem.*, 1999, **21**, 131.